A Dihydropyridine-sensitive Voltage-dependent Calcium Channel in the Sarcolemmal Membrane of Crustacean Muscle

Christian Erxleben*‡ and Werner Rathmayer*

From the *Department of Biology, University of Konstanz, D-78434 Konstanz, Germany; and ‡Stazione Zoologica 'Anton Dohrn,' Villa Comunale, I-80121 Naples, Italy

ABSTRACT Single-channel currents through calcium channels in muscle of a marine crustacean, the isopod *Idotea baltica,* were investigated in cell-attached patches. Inward barium currents were strongly voltage-dependent, and the channels were closed at the cell's resting membrane potential. The open probability (P_o) increased e-fold for an 8.2 mV (±2.4, $n = 13$) depolarization. Channel openings were mainly brief (<0.3 ms) and evenly distributed throughout 100-ms pulses. Averaged, quasimacroscopic currents showed fast activation and deactivation and did not inactivate during 100-ms test pulses. Similarly, channel activity persisted at steadily depolarized holding potentials. With 200 mM Ba^{2+} as charge carrier, the average slope conductance from the unitary currents between +30 and +80 mV, was 20 pS (±2.6, $n = 12$). The proportion of long openings, which were very infrequent under control conditions, was greatly increased by preincubation of the muscle fibers with the calcium channel agonist, the dihydropyridine Bay K8644 (10–100 μM). Properties of these currents resemble those through the L-type calcium channels of mammalian nerve, smooth muscle, and cardiac muscle cells.

KEY WORDS: single channel • arthropod

INTRODUCTION

The action potential in crustacean muscle fibers, originally shown by Fatt and Katz (1953) to be sodium independent, was later demonstrated to be carried by calcium ions (Fatt and Ginsborg, 1958; Hagiwara and Naka, 1964; Hencek and Zachar, 1977). Subsequently, it became clear that Ca action potentials are a general feature of arthropod muscle (adult insect muscle: Washio, 1972; larval insect muscle: Deitmer and Rathmayer, 1976; scorpion muscle: Gilly and Scheuer, 1984). Much as in vertebrate cardiac muscle, the voltage-dependent Ca^{2+} influx across the sarcolemmal membrane is necessary to elicit contractions in muscles of crustaceans (Zacharová and Zachar, 1967; Gainer, 1968; Hagiwara et al., 1968; Hidalgo et al., 1979; Mounier and Goblet, 1987) and other arthropods (Gilly and Scheuer, 1984). The influx of Ca^{2+} through the surface Ca channels alone, however, is insufficient for excitation-contraction coupling (Mounier and Goblet, 1987). As in vertebrate cardiac muscle, Ca^{2+} for the contraction of crustacean muscle comes primarily from a calcium-induced Ca^{2+} release (CICR) (Fabiato, 1985; Goblet and Mounier, 1986; Lea and Ashley, 1989; Györke and Palade, 1992).

In contrast to vertebrate cardiac muscle, smooth muscle and developing skeletal muscle, where the underlying single-channel Ca currents have been identified and characterized in great detail, crustacean muscle — or, for that matter, arthropod muscle — is poorly characterized with regard to the type and properties of single-channel Ca currents. Exceptions are a study on single-channel Ca currents in cultured embryonic *Drosophila* skeletal muscle fibers (Leung and Byerly, 1991), and a report on a dihydropyridine-sensitive Ca channel isolated from T-tubules of crayfish skeletal muscle and incorporated into lipid bilayers (Hurnák et al., 1990). Also in crayfish skeletal muscle, the modulation of Ca channels in the sarcolemmal membrane by the neuropeptide proctolin was described (Bishop et al., 1991).

The fundamental importance of Ca channels for calcium-induced Ca^{2+} release in crustacean muscle and the channel's function as a possible target for modulation of contractions by peptides and biogenic amines is in contrast to the scarcity of information on the single-channel's properties. In the present study, we characterize single-channel Ba currents in the sarcolemmal membrane of a crustacean muscle and show that they resemble Ca channels in vertebrate cardiac muscle and other vertebrate L-type channels.

MATERIALS AND METHODS

Preparation

Fast contracting fibers from abdominal extensor muscles of the marine isopod *Idotea baltica* (Crustacea, Isopoda) are particularly well suited for single-channel recordings because they are largely

A preliminary report of portions of this work has been previously published in abstract form (Erxleben, C. 1993. *Biophys. J.* 64:A149).

Address correspondence to Christian Erxleben, Stazione Zoologica 'Anton Dohrn,' Villa Comunale, I-80121 Naples, Italy. Fax: 039-81-7641-355; E-mail: erxleben@alpha.szn.it

free of connective tissue and accessible for patch-clamp recordings after modest enzymatic treatment. A detailed description of the preparation and the arrangement of the muscles were published previously (Erxleben et al., 1995). Patch-clamp recordings were performed in a small bath (0.5 ml vol) mounted on the stage of an inverted microscope (ZEISS IM, Oberkochen, Germany) at 400× magnification. Experiments were done at room temperature (20–25°C).

Electrophysiological Techniques and Data Analysis

Standard electrophysiological techniques were used for potential recording and current injection under current-clamp conditions (Erxleben et al., 1995). For two-electrode voltage-clamp experiments, an Axoclamp 2B (Axon Instruments Inc., Foster City, CA) was used. These experiments were performed on fibers of the last abdominal segment which are compact (270–450 μm long with a diameter of 50–80 μm). Injection of current in the middle of the fibers and recording at several points over the length of the fiber showed that they are isopotential and thus suitable for two-electrode voltage-clamp. For isolation of Ca or Ba currents and suppression of K currents, a solution (TEA solution) consisting of 160 mM tetraethyl-ammonium, 2 mM 4-aminopyridine (4-AP), 320 mM NaCl, 8 mM KCl, 20 mM HEPES, pH 7.4, was used with either 10 mM $CaCl_2$ or $BaCl_2$. In addition, the recording and current electrodes were filled with 3 M CsCl to suppress K currents. Voltage-activated Ca or Ba currents were separated from linear ionic and capacitive currents using a P/4 subtraction protocol.

Patch electrodes were fabricated from borosilicate glass (CLARK Electromedical Instruments, Reading, UK) coated with Sylgard 184 elastomer (Dow Corning Corp., Indianapolis, IN) to reduce noise. The electrodes were filled with high Ba^{2+} solution consisting of 200 mM $BaCl_2$, 150 mM TEA, and 20 mM HEPES. The pH was adjusted to 7.4 with $Ba(OH)_2$. The bath contained artificial sea water (ASW)[1] consisting of 490 mM NaCl, 8 mM KCl, 10 mM $CaCl_2$, 12 mM $MgCl_2$, and 20 mM Tris, pH 7.4. Single-channel currents were recorded with an EPC-7 patch-clamp amplifier (List Electronic, Darmstadt, Germany) in the cell-attached configuration.

Pulse protocols and data acquisition were controlled by an interface (CED1401, CED, Cambridge, England for the patch-clamp experiments, and DigiData 1200, Axon Instruments for the current- and voltage-clamp experiments) connected to an IBM-compatible personal computer. Data were analyzed with software of the CED patch and voltage-clamp suite or PCLAMP software (Axon Instruments). Single-channel currents were low-pass filtered at 20 kHz, digitized by a modified PCM adapter (Sony) and stored on video tape. For analysis and preparation of figures, the data were re-filtered with a hardware 8-pole bessel filter with a cut-off frequency of 3 kHz (−3 db). Alternatively, a variable software implementation of a Gaussian filter (PCLAMP software) was used. Data were digitized at a sampling frequency of at least five times the filter frequency. Single-channel currents elicited by depolarization up to 60 mV from the resting membrane potential were analyzed after 3 kHz filtering. For larger depolarization 2 or 1 kHz filtering was used, depending on the signal-to-noise ratio of the recordings. The 3 kHz Gaussian filter, equivalent to a 10–90% rise time (t_r) of 100 μs, limits the detection of channel openings to 0.6 times t_r, or 60 μs and currents larger than about two times t_r, or 200 μs, should be of unattenuated amplitude (Colquhoun and Sigworth, 1983). The choice of a 3 kHz filter is a compromise between acceptable time resolution and an acceptable proportion of spurious events caused by excessive baseline noise. The frequency of channel openings at +50 mV was only in the order of 10/s and the rate of false openings due to noise should be at least one to two orders of magnitude smaller than the opening rate (Colquhoun and Sigworth, 1983). For a recording at +50 mV from the resting potential with current amplitudes of ~1 pA, this implies a ratio of 5 between current amplitude and RMS baseline noise, which, for a typical recording at +50 mV, was achieved with a 3 kHz filter (between 0.15 and 0.2 pA RMS noise).

Steady-state open probabilities (P_o) were determined from patches with at most three active channels by summation of the channel open times of all levels divided by the number of channels in the patch and the recording time. The number of channels in a patch (N) was judged by the maximum number of simultaneously open channels at depolarization of 80–100 mV from rest. For voltage steps, P_o values of 4–16 sweeps (100 ms) were averaged, and P_o values of channel activity during maintained depolarization were determined during 2–30 s periods, depending on the opening frequency of the channels. P_o values were only calculated from periods of uniform channel activity, while any times during which there was an obvious change to low or zero activity were excluded (see Fig. 11).

For the preparation of the figures and calculation of averaged, quasimacroscopic currents, leak and capacitive currents were subtracted from the single-channel current records during voltage steps. This was achieved by adding averaged current records of negative pulses (which did not elicit any currents) to the test pulse current records. Since the leak-subtraction procedure introduces additional noise, P_o values, single-channel current amplitudes and kinetics derived from voltage-step experiments were determined from the raw data.

Potentials are referred to as holding potential (HP) relative to the membrane resting potential, or as membrane potential (V_m), in which case a resting potential of −70 mV is assumed. This is the average resting potential determined in earlier experiments with intracellular electrodes (Erxleben et al., 1995). As for conventional intracellular voltage recordings, potentials are always expressed relative to the exterior face of the membrane. Inward currents are shown as downward deflections.

Average values are given as mean ± standard deviation with n referring to the number of patches in the case of single-channel recordings, and the number of fibers in the current- and voltage-clamp experiments.

RESULTS

When abdominal extensor twitch muscle fibers of *Idotea baltica* are depolarized by injection of constant current under physiological conditions (i.e., in ASW), a graded active electrical response is usually elicited, rather than an action potential (Erxleben et al., 1995). After application of 10 μM Bay K8644, a dihydropyridine (DHP) agonist of L-type Ca channels, this graded response was converted into an action potential (Fig. 1 *A*). Subsequent application of 10 μM nifedipine, an antagonist of L-type Ca channels, reduces the action potential again to a graded response (Fig. 1 *A*), ($n = 2$). If K currents were suppressed by including TEA and 4-AP in the extracellular solution (TEA solution, see MATERIALS AND METHODS), the fibers responded to suprathreshold depolarizing current pulses with action potentials. This response is well known from other crustacean muscle fibers (Fatt and Katz, 1953; Fatt and Ginsborg, 1958).

[1]*Abbreviations used in this paper:* ASW, artificial sea water; DHP, dihydropyridine.

The duration of the action potentials, defined as time between maximal rate of rise and fall, ranged from 90–200 ms in Ca^{2+} solution (10 mM) and was greatly increased ($n = 4$) to between 5.1 and 32 s in Ba^{2+} solution (Fig. 1, *B* and *C*). Since most voltage-dependent K currents, in particular Ca^{2+}-activated K currents, should be blocked in the TEA solution (Araque and Buño, 1995; Gielow et al., 1995), the much longer action potentials in Ba^{2+} solution than in Ca^{2+} solution suggests that the duration of the Ca spike is at least in part determined by calcium-dependent inactivation. Spikes in TEA solution were blocked by 20 μM nifedipine (data not shown, $n = 3$).

The difference in inactivation between Ca and Ba currents ($n = 4$ and 5) is evident from the currents measured under voltage-clamp (Fig. 1 *D*). Whereas the decay of the Ca current includes a fast component of inactivation, the Ba current inactivates more slowly. The Ba current was reduced by nifedipine ($n = 3$), as expected from the block of the action potential, and completely blocked by 100 μM Cd^{2+} ($n = 5$), (Fig. 1, *E* and *F*). The most obvious effect of 10–50 μM Bay K8644 on the Ba current was a large increase in the tail currents (Fig. 1 *F*, $n = 3$), which were very brief and small in the absence of the drug (Fig. 1, *D* and *E*).

While the properties of the Ca and Ba currents in *Idotea* muscle fibers are merely illustrated here (a detailed analysis is to be published elsewhere), the converse effects of the L-type Ca channel modulators on Ca and Ba action potentials and currents clearly suggest the presence of L-type Ca channels in crustacean muscle and prompted us to characterize the single-channel currents underlying the active electrical responses in *Idotea* muscle fibers.

In cell-attached patches with Ba^{2+} solution in the pipette and normal saline in the bath, no channel activity was seen at the cell's resting potential. Only when the patch was depolarized by voltage steps of 20–30 mV could very brief (100–300 μs) and infrequent inward currents be observed. Inward currents became smaller in amplitude but much more frequent with further depolarization (Fig. 2 *B*). Single-channel openings were uniformly distributed throughout the pulses, indicating that there is little inactivation during the 100-ms test pulses (Fig. 2 *B*).

To directly compare the single-channel Ba currents to macroscopic currents reported from this (Fig. 1) and other crustacean and arthropod preparations, we averaged single-channel currents that were elicited during voltage steps (see Fig. 2 *B*). The averaged and leak-subtracted, quasimacroscopic Ca currents showed fast activation and deactivation with no inactivation during the 100-ms pulses (Fig. 2 *C*). The averaged currents were highly voltage-dependent and reached a maximum at 90 mV depolarization (Fig. 2 *D*).

Single-channel Amplitude and Conductance

All-point histograms (Fig. 3 *A*) were used to estimate the single-channel current amplitudes, and the 50%

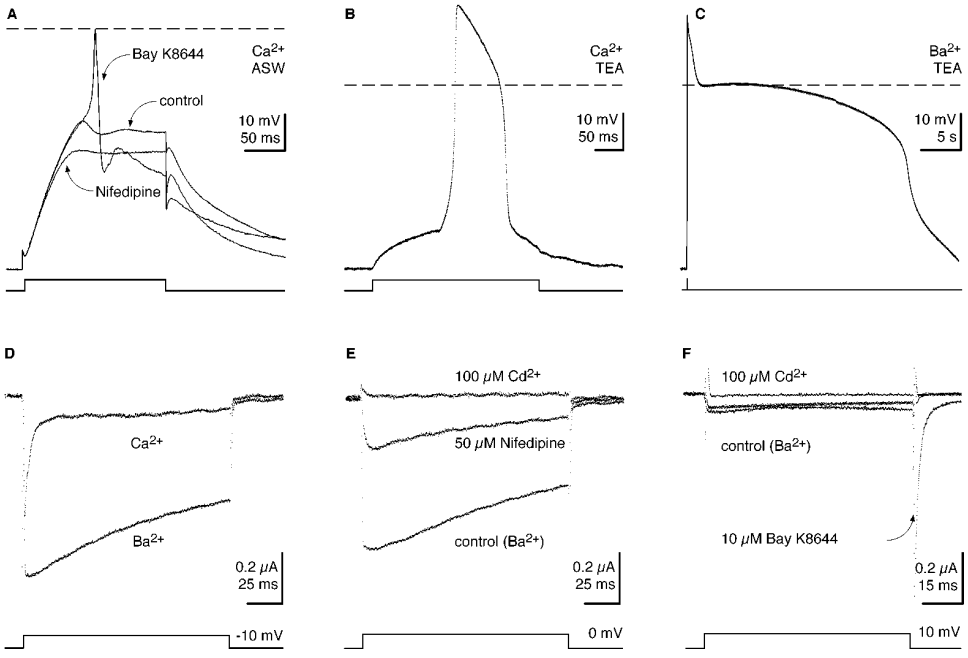

FIGURE 1. Active membrane responses and inward currents in *Idotea* muscle fibers. (*A*) Active membrane responses (graded) elicited by constant current pulses under control conditions, 20 min after application of 10 μM Bay K8644 (action potential), and 20 min after subsequent application of 10 μM nifedipine (graded). Experiment in artificial sea water, resting potential −70 (±2) mV. (*B*) Ca spike elicited by a constant current pulse in TEA-ASW and (*C*) after substituting Ba^{2+} as charge carrier. Resting potentials were −56 mV for *B* and −53 mV for *C*. The dashed lines indicate 0 mV membrane potential. (*D*) Ca and Ba currents elicited by voltage clamp steps. (*E*) Suppression of Ba currents by nifedipine and Cd^{2+}. (*F*) Ba current under control conditions (*middle trace*), in the presence of Bay K8644 and after block by Cd^{2+}. Linear leak and capacitive current were subtracted, see MATERIALS AND METHODS. Holding potential for all records was −80 mV. Current records in *D* and *E* are from the same muscle fiber.

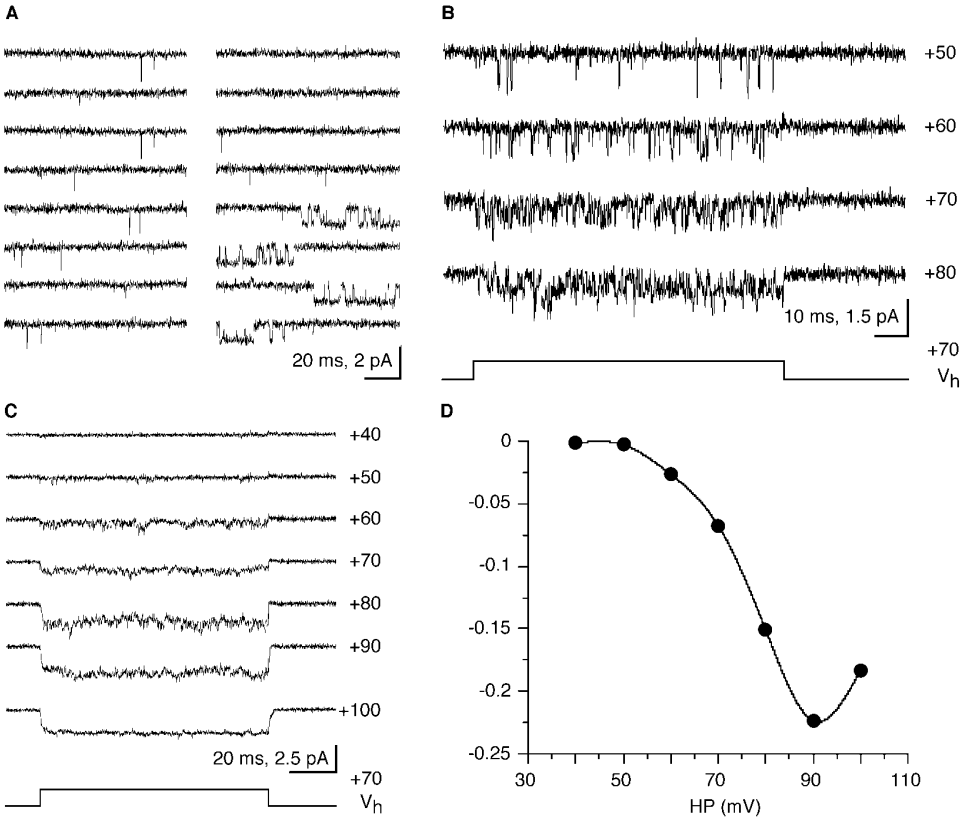

FIGURE 2. Single-channel Ba currents are activated by depolarization. (*A*) Continuous record (1.7 s) from a patch held at +40 mV from the resting potential shows the typical brief channel openings and two bursts of long openings (*right*). (*B*) Capacity- and leak current–subtracted single-channel currents which were elicited by depolarizing voltage steps. (*C*) Quasi-macroscopic currents obtained from averaged, leak-subtracted single-channel current traces elicited by voltage jumps like those in *B*. Between 8 and 16 records were averaged. (*D*) Current integrals (charge) from *C* plotted as a function of the depolarization. Potentials shown along each trace (*B* and *C*) indicate the depolarization reached during 70-mV steps of 100 ms duration that were applied from different holding potentials. All potentials are relative to the cells' resting membrane potential. Cell-attached were patches from different cells.

value of the amplitude was used for setting the detection threshold of the analysis program. The single-channel conductance of the channel was determined from distributions of the idealized single-channel current amplitudes as measured by the analysis program, to which Gaussian distributions were fitted (Fig. 4 *A*). To exclude data from attenuated openings, only amplitude values of openings longer than twice the rise time of the filter (t_r) were included in these plots (see MATERIALS AND METHODS). A combined plot of all single-channel current-voltage relationships would have a lot of scatter due to differences in the resting potential. We therefore show a representative plot of single-channel current amplitude as a function of depolarization from one patch (Fig. 4 *B*). The mean conductance with 200 mM Ba^{2+} as charge carrier was 20 ± 2.6 pS (n =

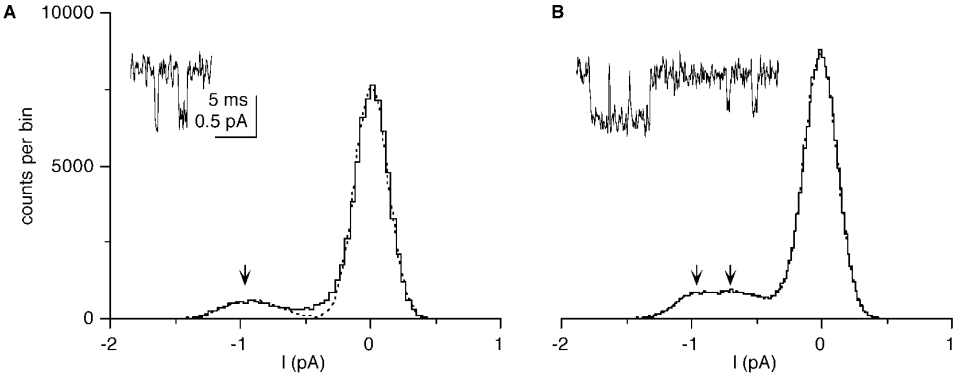

FIGURE 3. All-point histograms of Ba currents were used to estimate the number of conductances and single-channel current amplitudes. (*A*) In the absence of the dihydropyridine Bay K8644, only one class of amplitudes is observed (*arrow*, 0.91 pA at +60 mV depolarization). (*B*) In the presence of 50 μM Bay K8644, two classes of amplitudes (*arrows*, 0.62 pA and 0.99 pA at +70 mV depolarization) can be resolved. The amplitudes were obtained from the best fit of the sum of two (*A*) or three (*B*) Gaussian distributions. The insets are typical sample traces showing currents of one (*A*) and two (*B*) amplitude classes respectively. Records were filtered at 2 kHz.

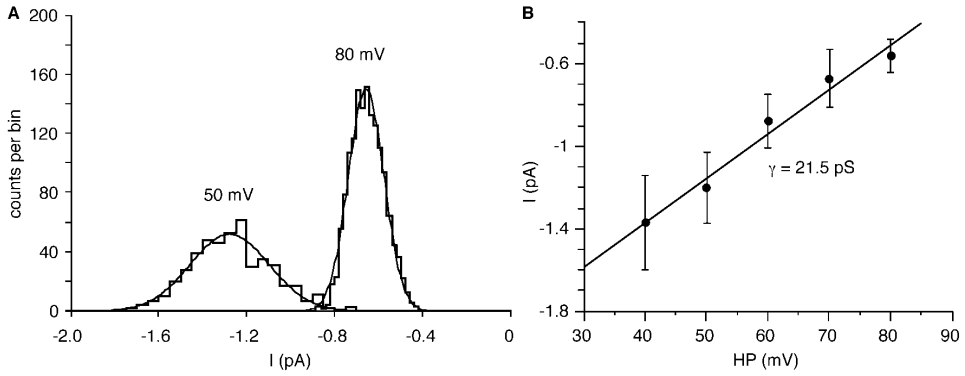

FIGURE 4. Current-voltage relationship for the Ca channel. Mean single-channel current amplitudes were determined from distributions of the measured current amplitude, which were fitted by Gaussian distributions. (*A*) Distributions of single-channel current amplitudes at +50 and +80 mV depolarization. (*B*) Single-channel conductance which was determined from linear least-squares fits of the mean single-channel current amplitudes. The error bars denote the standard deviation of the Gaussian fits. All potentials are relative to the cell's resting membrane potential.

12). A linear extrapolation from the single-channel amplitude plots to zero current gave an average apparent reversal potential of +112 ± 15 mV (n = 12). With a resting potential of −70 mV, the average value measured previously with intracellular microelectrodes (Erxleben et al., 1995), current reversal occurs at an absolute membrane potential of +42 mV. Because of the highly asymmetric Ba^{2+} distribution under our recording conditions, a pronounced inward rectification is predicted by the constant field theory (Hodgkin, 1951). Thus, a linear extrapolation will underestimate the true reversal potential. A probably more realistic value for the reversal potential, +73 mV (absolute), was directly obtained from averaged, leak-subtracted single-channel currents that were recorded from multi-channel patches during 150-mV voltage ramps (Fig. 5, *A* and *B*). Care was taken to exclude traces with any contaminating outward potassium currents which would again bias the current reversal potential towards more negative values.

Because all recordings of the single-channel currents were done in the cell-attached configuration, the ion selectivity of the channels could not be determined individually and for the same patch. Experiments with either artificial sea water or high potassium solution (Erxleben et al., 1995) in the patch pipette, however, never showed any single-channel currents of comparable voltage range of activation, single-channel conductance, or channel dwell times. Thus, it appears that the observed Ba currents were through real Ca channels rather than nonselective cation channels.

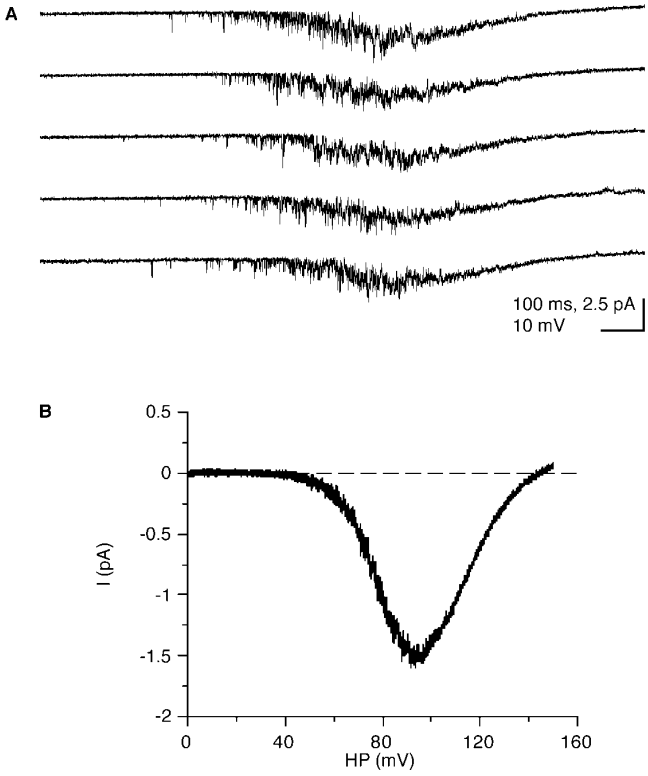

FIGURE 5. Single-channel Ba currents elicited by voltage ramps in a multi-channel patch. (*A*) Individual current traces elicited by 150-mV voltage ramps (1 s duration) from the resting potential. (*B*) Average of 16 records after leak subtraction. The leak, equivalent to a seal resistance of 290 GΩ, was determined from the slope of the initial part of the records which showed no channel openings (0–25 mV) in any of the averaged traces. A fit of a Boltzmann curve of the type $I_{max.}/\{1 + \exp[(V_h - HP)/k]\}$ to the current below the peak of the I-V curve (up to 80 mV depolarization) gave a slope k of + 8.4 mV (for an e-fold change in current), +80 mV for the half-maximal activation V_h of the current, and −2.1 pA for $I_{max.}$. Experiment in the presence of 50 μM Bay K8644.

Evidence for the Presence of Just One Channel Type

Since previous studies of single-channel Ba currents in the crayfish (Bishop et al., 1991) and *Drosophila* muscle (Leung and Byerly, 1991) and more recently of macroscopic Ba currents in *Drosophila* muscle (Gielow et al.,

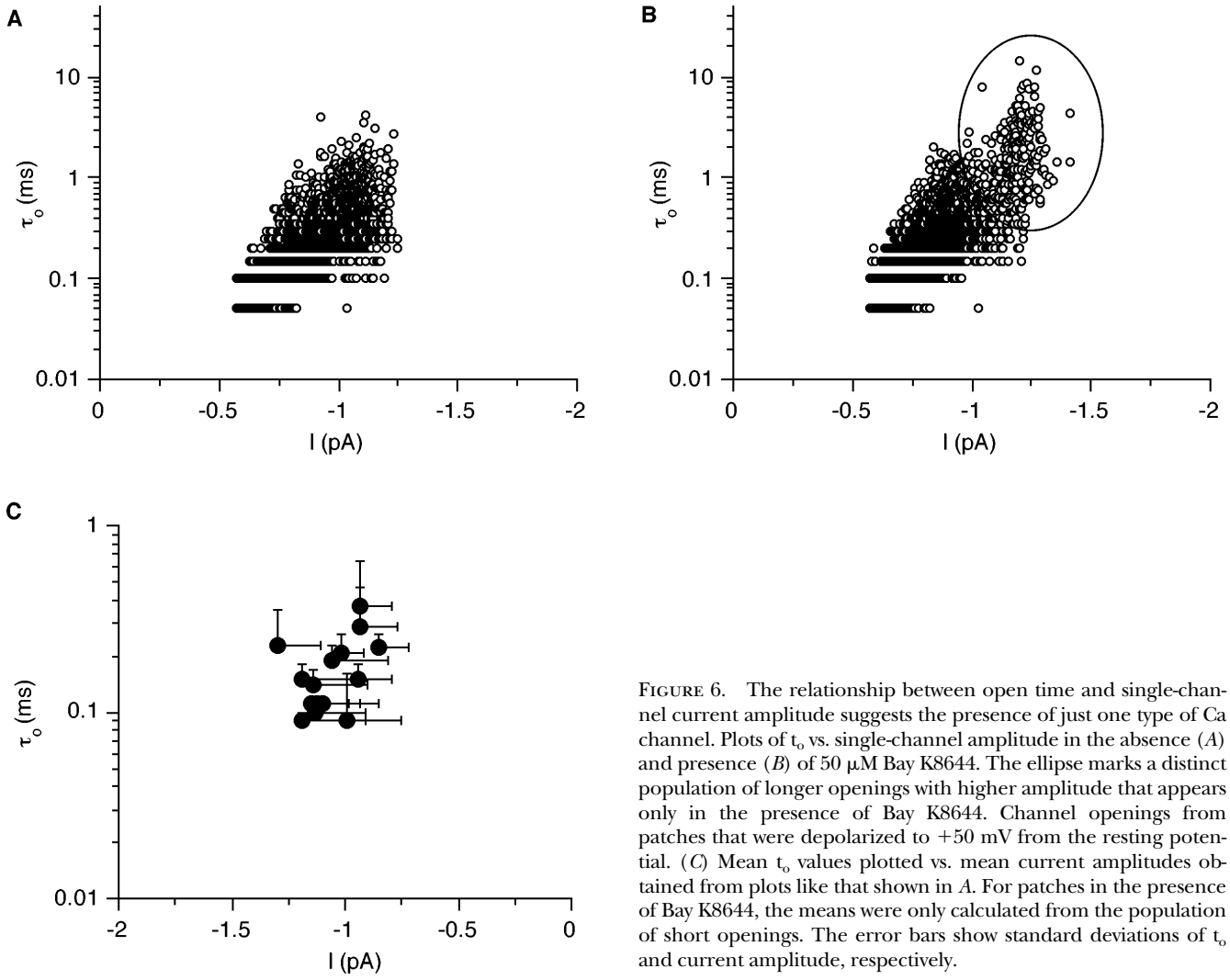

FIGURE 6. The relationship between open time and single-channel current amplitude suggests the presence of just one type of Ca channel. Plots of t_o vs. single-channel amplitude in the absence (*A*) and presence (*B*) of 50 μM Bay K8644. The ellipse marks a distinct population of longer openings with higher amplitude that appears only in the presence of Bay K8644. Channel openings from patches that were depolarized to +50 mV from the resting potential. (*C*) Mean t_o values plotted vs. mean current amplitudes obtained from plots like that shown in *A*. For patches in the presence of Bay K8644, the means were only calculated from the population of short openings. The error bars show standard deviations of t_o and current amplitude, respectively.

1995) suggest the presence of more than one type of Ca channel in arthropod muscle, we had to establish that there is really only one type of Ca channel in our records. This was particularly important since many channel openings were brief at threshold depolarization and, due to the frequency limitations, attenuated in amplitude. Therefore, we analyzed channel openings by plotting the relationship between current amplitude and open time. Such plots show a single cluster of data points. As an example, data from currents elicited by maintained 50 mV depolarization are shown in Fig. 6 *A*. Particularly for the open times in the first two bins (50 and 100 μs) there is a tendency for larger currents to be of longer duration, which is what we expect due to the frequency limitations. There is, however, no indication of a second distinct cluster which would suggest the presence of another channel type. The same plots were analyzed for 14 other patches that lasted long enough to allow a quantitative evaluation. The summary (mean open time at 50 mV depolarization in relation to mean current amplitude) is plotted in Fig. 6 *C*.

Channel Open Times

At threshold depolarization (20–30 mV from the resting potential) channel openings were in the order of 100 μs, and many openings did not reach full amplitude with the bandwidth of 3 kHz that was required for an adequate signal-to-noise ratio of our recordings. The channel's gating was analyzed in continuous records during maintained (5–30 s) depolarization (Figs. 2 *A* and 7 *A*) during which there was no indication of a time-dependent decrease in single-channel activity (see *Modal Gating*). At depolarization of 40 mV and higher, longer openings (milliseconds in duration) were occasionally observed (Fig. 2 *A*), although most openings were still in the 100–300 μs range. Consequently, open time distributions could be reasonably well fitted by a single ex-

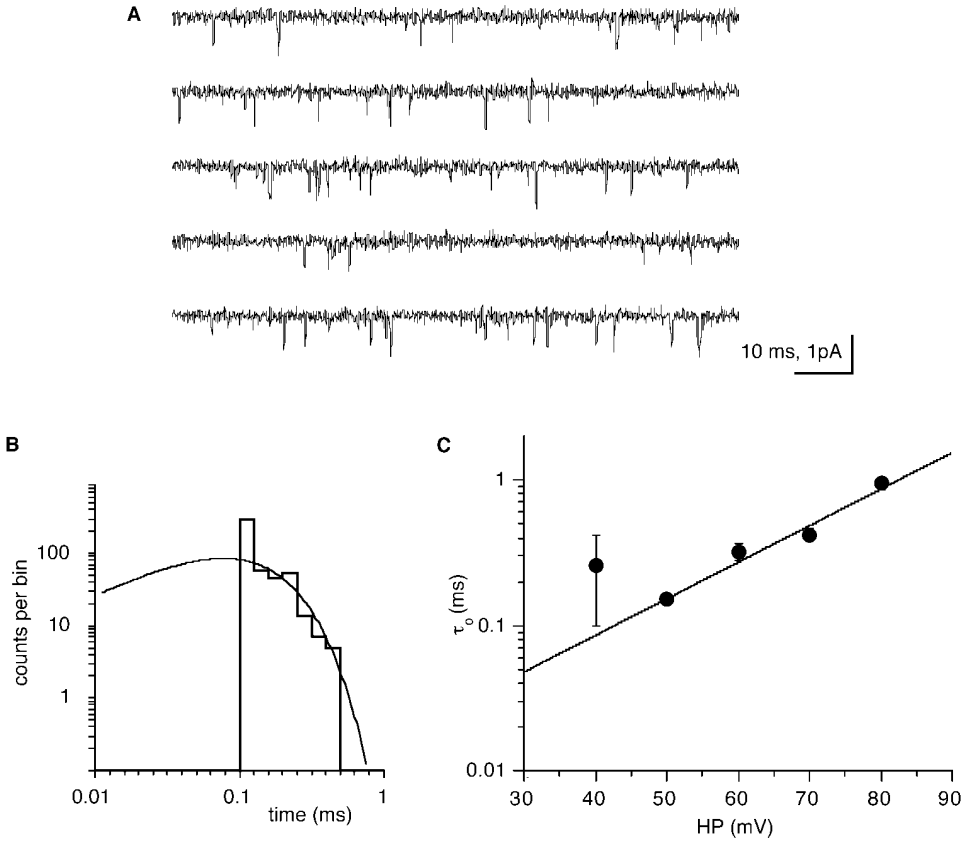

FIGURE 7. Open times of the Ca channel follow a single exponential function which increases with depolarization. (*A*) Continuous record (0.5 s) of single-channel activity at steady depolarization to +50 mV, relative to the cell's resting membrane potential. (*B*) Open time distribution at +50 mV depolarization with the log-log plot fitted by a time constant of 0.16 ms. (*C*) Mean open times of the channel as a function of the depolarization. The error bars show the standard error of the individual fits, and the straight line is a weighted least-squares exponential fit to the data points.

ponential component (Fig. 7 *B*) since long openings, if present at all, were much too infrequent to contribute to the distributions. Channel open times increased with depolarization (Fig. 7 *C*).

Voltage Dependence of the Channel's Open Probability

The dependence of the channel's opening probability on the membrane potential (see Fig. 2) was investigated quantitatively in patches with, at the most, three active channels, as judged from the maximum number of simultaneously open channels at depolarization of 80–100 mV from rest. While the probability of finding channels in any given patch was quite low (5–10%), the open probability of the channel at large depolarization was high, unless in the silent mode (see *Modal Gating*). The average P_o was 0.15 ± 0.08 (n = 12) at 80 mV, 0.34 ± 0.13 (n = 7) at 90 mV and 0.55 ± 0.07 (n = 5) at 100 mV depolarization. Open probabilities (P_o) were determined from two types of protocols: during voltage steps (Fig. 2 *B*) and during maintained depolarization (Figs. 2 *A* and 7 *A*). An example of a P_o vs. holding potential plot is shown in Fig. 8, including data from steady depolarization and voltage steps. With the exception of P_o values at steady 20 and 30 mV depolarization, there is good agreement between values obtained with the two methods. At 20 and 30 mV depolarization, most channel openings are probably so brief that they are filtered down to <50% amplitude by the 3 kHz upper frequency limitation. Consequently, these events escape the detection threshold and hence the apparent P_o value is lower than expected from the fitted Boltzmann curve of the remaining data (Fig. 8). The average voltage sensitivity, i.e., the depolarization necessary for an e-fold change in P_o, from this type of plot was +8.2 ± 2.4 mV (n = 13). Half-maximal activation ($V_{0.5}$) of the Ca channel required 89.3 ± 12.4 mV (n = 13) depolarization.

Very similar values for the voltage sensitivity (8.4 mV for an e-fold change in Ca current) and half-maximal activation (80 mV for $V_{0.5}$) were obtained from averaged currents elicited during voltage ramps (Fig. 5, *A* and *B*) in the presence of the dihydropyridine Bay K8644 (see below). The voltage dependence of the averaged (leak-subtracted) ramp currents was calculated by fitting a Boltzmann-type equation to the ascending part of the I-V relationship (Fig. 5 *B*). The fit was restricted to the potential range where the single-channel I-V relationship was linear (Fig. 4 *B*), and a fit does not require that the constant-field rectification be taken into account.

Dihydropyridine Sensitivity

After preincubation of the preparation with the dihydropyridine Bay K8644, an agonist of L-type Ca channels in vertebrate muscle and neurons (see, e.g., Bechem

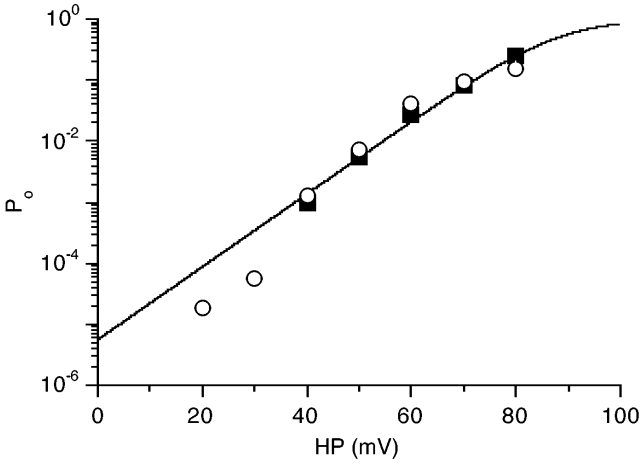

FIGURE 8. Open probability of the Ca channel increases strongly with depolarization. Plot of P_o as a function of the membrane potential in a patch with one active channel. P_o values were determined during steady depolarization (*open circles*) or from voltage steps (*closed squares*) to the indicated potentials. The curve through the data points is a fit to a Boltzmann curve with $P_o = 1/\{1+ \exp [(V_h - HP)/k]\}$ where V_h is the depolarization necessary for half-maximal channel activation (+88 mV), *HP* the patch potential (relative to rest), and *k* the depolarization necessary for an e-fold change in P_o (+7.2 mV). The values for steady 20 and 30 mV depolarization are not included in the fit (see RESULTS).

et al., 1988), long channel openings, which were very infrequent in the absence of the drug, became apparent during either 100-ms voltage steps (Fig. 9 *A*) or continuous depolarization (Figs. 9 *B* and 10 *A*). As a consequence of the increased frequency of long openings in the presence of Bay K8644, open time histograms show a distinct second component with a time constant in the millisecond range (Fig. 9 *C*).

Concentrations of 10–100 μM Bay K8644 induced long openings while 1 μM had no effect. No systematic difference was observed between concentrations of 10–100 μM, possibly due to a limited solubility of Bay K8644. In experiments with Bay K8644 which showed a particularly high frequency of long openings, such as shown in Fig. 10 *A*, it became apparent that the single-channel current amplitudes of the long openings were larger than those of the short openings. While the all-point histograms and the measured amplitude distributions in the absence of Bay K8644 clearly contained only one class of amplitudes (Figs. 3 *A* and 4 *A*), the all-point histograms show a second component in the presence of Bay K8644 (Fig. 3 *B*). Likewise, the histograms of measured amplitudes showed a second distinct, larger peak (Fig. 10 *B*). Similarly, the relationship between open time and amplitude showed a second

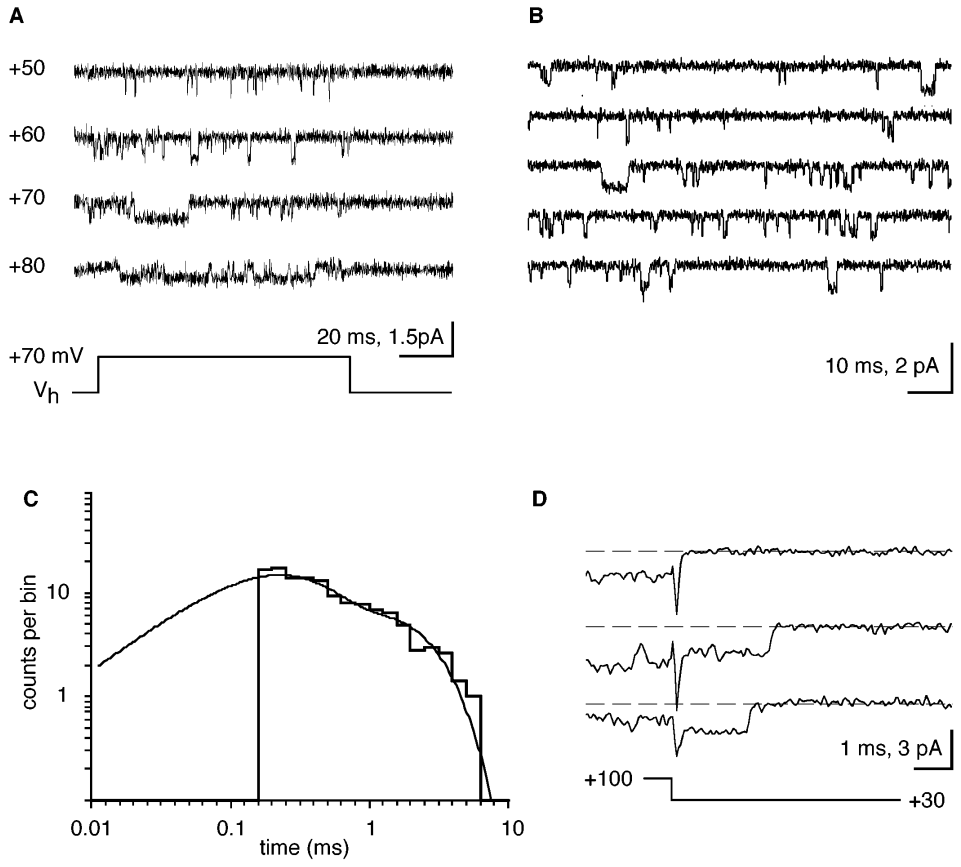

FIGURE 9. The dihydropyridine Bay K8644 promotes long openings of the Ca channel. (*A*) Single-channel currents elicited by depolarizing voltage steps. Potentials shown along each trace indicate the depolarization reached during 70-mV steps of 100 ms duration that were applied from different holding potentials. (*B*) Continuous record (0.5 s) of single-channel activity at steady depolarization to +50 mV. All potentials are relative to the cell's resting membrane potential. (*C*) Open time distribution at +50 mV depolarization with the log-log plot fitted by the sum of two exponentials with time constants of 0.16 and 0.8 ms. Experiment in the presence of 50 μM Bay K8644. (*D*) Tail currents elicited by voltage jumps +100 mV from the resting potential to +30 mV from rest. Leak-subtracted records from a patch in the presence of 50 μM Bay K8644 with three consecutive traces (100-ms jumps every 6 s) of which one (*top trace*) shows no tail currents. Current records filtered at 2 kHz.

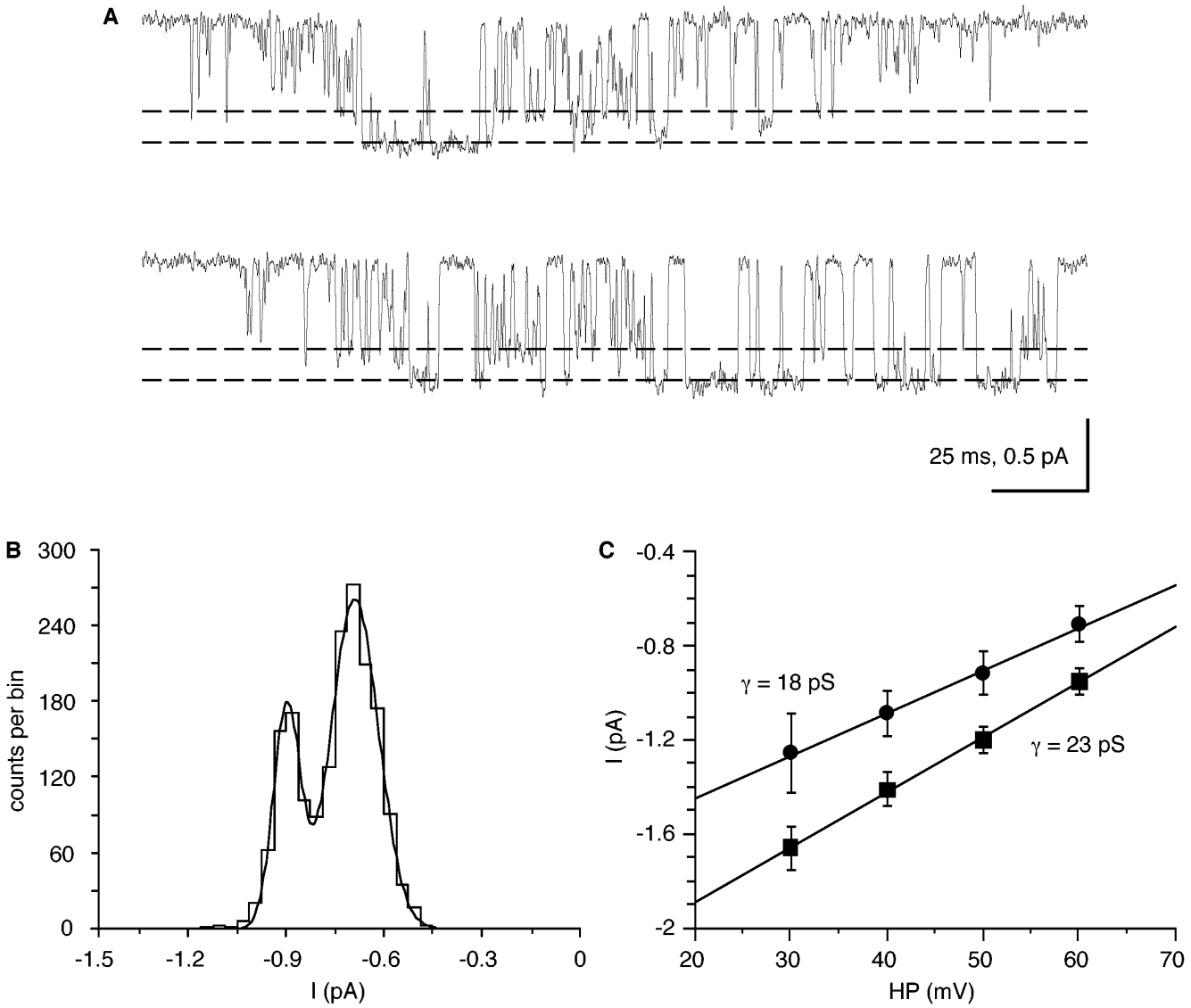

FIGURE 10. Multiple conductance levels in the presence of Bay K8644 (50 μM). (*A*) Two sample records (0.25 s) during steady +60 mV depolarization which show large amplitude long-duration openings and short-duration openings of smaller amplitude. The dashed lines indicate the two conductance levels of the open channel. Records were filtered at 1.5 kHz. (*B*) Distribution of single-channel current amplitudes at +60 mV depolarization, fitted by the sum of two Gaussians. (*C*) Plot of single-channel conductances which were determined from linear least-squares fits of the mean single-channel current amplitudes. The error bars denote the standard deviation of the Gaussian fits. All potentials are relative to the cell's resting membrane potential.

cluster in the presence of Bay K8644 (Fig. 6 *B*). In other experiments, where the frequency of long openings was lower, amplitude distributions only showed a slight skew towards larger amplitudes or a shoulder in the distribution (data not shown).

From the quasimacroscopic, averaged single-channel records it is obvious that the current deactivates very fast (Fig. 2 *C*). In the single-channel records this shows in the absence of tail currents, i.e., channel openings after the repolarizing voltage step. In the presence of Bay K8644, however, we observed tail currents in voltage step experiments (Fig. 9 *D*), presumably because the rate of deactivation is slowed in the presence of Bay K8644.

We did not see an effect of Bay K8644 on the voltage sensitivity of the Ca channel reported for L-type Ca currents and channels in other preparations (see DISCUSSION). There was no significant difference in the voltage sensitivity, which was 7.9 ± 2.9 mV (n = 7) without Bay K8644, and 8.5 ± 2.0 (n = 6) from patches with 25–100 μM Bay K8644. Similarly, no significant difference was found in the potential of half-maximal activation of the channel with or without Bay K8644 (85 ± 11 mV, n = 6 and 93 ± 13 mV, n = 7, respectively).

For a more complete pharmacological characterization of the channels it would of course be helpful to study the effects not only of the DHP agonist Bay K8644 but also of DHP antagonists, such as nifedipine or nitrendipine and peptides of the conotoxin family. DHP antagonists are presumably membrane permeant and could thus be applied to the bath while recording in the cell-attached configuration. The spontaneous switching of the Ca channels between silent and active mode (see *Modal Gating*), however, combined with the long time the DHPs require to exert their effects in this preparation, make the interpretation of changes in activity of the channels inherently difficult. Fast acting toxins and channel blockers like Cd^{2+} require application to the external face of the membrane and cannot be easily applied in the cell-attached configuration. Preliminary attempts to obtain outside-out patches were promising in that we could get channels in this configuration. There was, however, rapid loss of activity of the channels that resembled the Ca channels found in the cell-attached mode. "Rundown" occurred even with Mg-ATP in the pipette and with Bay K8644 in the bath — conditions which slow the rundown of whole-cell Ca currents and single-channel activity of L-type Ca channels in many cells (see Bean, 1992).

Modal Gating

The complete absence of inactivation of either single-channel currents (Figs. 2 *B* and 9 *A*) or quasimacroscopic currents (Fig. 2 *C*) during 100-ms voltage steps prompted us to look at channel activity during extended periods. Even during several seconds of depolarization, there is no inactivation of the single-channel Ba currents. This is demonstrated in a plot of open probability versus time (Fig. 11 *A*). If the activity is observed over even longer times (minutes), spontaneous changes between periods of activity and periods with no or very few openings become apparent (Fig. 11 *B*), indicating different modes of gating.

If we look at the open probability over time in the absence of Bay K8644 we find that, with the exception of periods during which the channel seems unavailable for opening, P_o values averaged over a 100-ms "sweep" are fairly homogeneous (Fig. 12, *A* and *B*) and appear as a single, approximately Gaussian distribution in P_o histograms (Fig. 12, *D* and *E*). The effect of stronger depolarization, i.e., from +60 to +70 mV leads to a shift of this distribution, towards higher P_o values, as expected due to the voltage sensitivity of the channel (Fig. 12 *E*). In the presence of Bay K8644, two changes in the plots of P_o over time become evident. The distribution of P_o values becomes broader, and there is a number of high P_o sweeps which are clearly from a different population. These high P_o sweeps consist mainly of long openings like the sample traces shown in Figs.

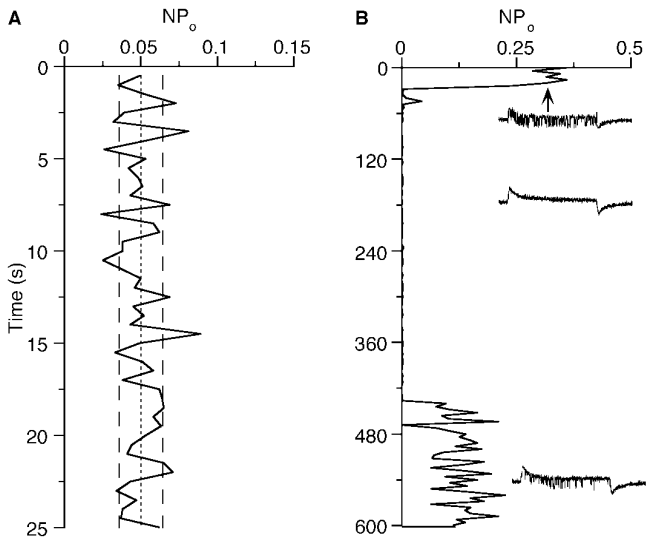

FIGURE 11. Ca channels in cell-attached patches do not inactivate but show clearly distinguishable periods of activity and inactivity. (*A*) The relative open probability (NP_o) determined from 0.5-s segments during steady depolarization to +50 mV. N is the number of channels in the patch. The lines indicate mean NP_o (*dotted*) and ± SD (*dashed*), respectively. (*B*) In another patch, NP_o was determined from voltage jumps (70 mV depolarizing jumps of 100-ms duration every 4 s) from the resting potential, which were recorded over a period of 10 min. During the first 30 s two channels were active, while only one channel was active during the last 3 min of the recording. Representative sample traces from the beginning, middle, and end of the recording are shown as insets.

9, *A* and *B*, and 10 *A*. In addition there is a tendency for clusters of long openings to occur. For the recording shown in Fig. 12, *C* and *F*, for example, the total probability of high P_o sweeps (defined as those with a $P_o \geq 0.5$) is 5%, and it is therefore unlikely that clusters of four or five consecutive high P_o sweeps, as can be seen in Fig. 12 *C*, will be observed by chance. Likewise, null P_o sweeps, which correspond to the first bins in the distributions (Fig. 12, *D–F*) appear in clusters, as can be seen in Fig. 12 *C* (between 15 and 19 s of the record).

DISCUSSION

Evidence for a Single Ca Channel Type

A detailed biophysical analysis of the Ca channels in *Idotea* muscle fibers presented here is hindered by the rapid kinetics and small amplitude of the Ca channel currents. At depolarization up to +50 mV (relative to the resting membrane potential) a significant proportion of openings is either not detected at all on the basis of the 50% threshold criterion, or remains poorly resolved. Therefore, we cannot exclude the possibility that some of these openings are from other than the DHP-sensitive Ca channel. The evidence for the presence of just one channel type, however, is as follows. (*a*) Plots

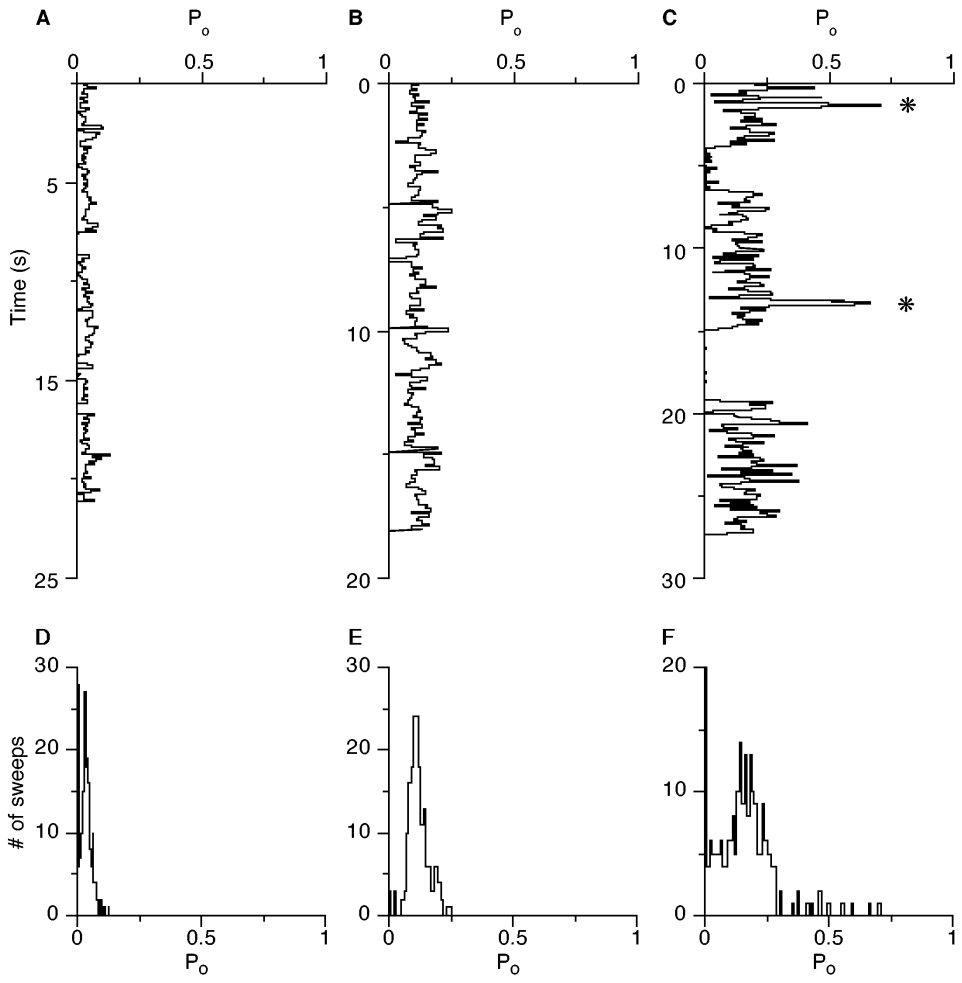

FIGURE 12. Effect of Bay K8644 on the open probability of the channel. Channel P_o of 100 ms segments from recordings at continuous depolarization plotted against time (*A–C*). (*D–F*) Histograms of P_o values for the periods shown in *A–C*. The first and probably second bin of each distribution represent segments with no detectable openings (28 and 6 in *D*, 3 and 0 in *E*, 63 and 4 in *F*). Recordings from a patch under control conditions at +60 mV (*A* and *D*) and +70 mV (*B* and *E*) and in the presence of 50 μM Bay K8644 (*C* and *F*) at +60 mV constant depolarization. The asterisks in *C* mark clusters with 4 and 5 consecutive high P_o sweeps (see text).

of open time vs. single-channel amplitude show only one cluster of data points and a distinct second cluster appears only in the presence of Bay K8644 (Fig. 6, *A* and *B*). (*b*) The combined distribution of open time vs. single-channel amplitude from all patches (Fig. 6 *C*) is fairly homogeneous, and provides no evidence for another population of channels. (*c*) Neither the quasi-macroscopic I-V curves from voltage-jump experiments (Fig. 2 *D*) nor those obtained with voltage-ramps (Fig. 5 *B*) show a "shoulder" or "bump" which would indicate the presence of another population of channels. If, however, different channel-types were to activate within the same range of potentials, as is the case for two Ca current components in *Drosophila* larval muscle (Gielow et al., 1995), this would not necessarily show in the I-V curves. (*d*) It could be argued that the long-duration openings represent another type of Ca channel that is rarely active in the absence of Bay K8644 and more frequently open in the presence of the drug. The fact is, however, that we recorded currents with brief and long openings (i.e., Figs. 9 *B* and 10 *A*) in patches that clearly showed no double openings even with strong depolarization (100 mV) where the average P_o was 0.55. This shows that the larger amplitude, long-duration openings actually represent another conformation of the same channel rather than a second channel type.

Finding two conductance levels in the presence of Bay K8644 (Fig. 10) is not unprecedented: multiple conductance levels in the presence of Bay K8644 have been reported for L-type Ca channels in cardiac muscle (Lacerda and Brown, 1989) and GH_3 cells (Kunze and Ritchie, 1990).

Comparison to Ca Channels in Other Arthropod Muscles

The only other arthropod muscle single-channel Ca currents described so far that seem similar to the currents we found in the sarcolemmal membrane of *Idotea* muscle fibers are those from cultured *Drosophila* myotubes (Leung and Byerly, 1991). These channels have a similar conductance (18.5 pS with 100 mM Ba^{2+} solution), show no inactivation during 90-ms test pulses, and, like the *Idotea* Ca channels, exhibit rapid kinetics (Leung and Byerly, 1991). *Drosophila* muscle Ca channels, however, resemble more closely the N-type Ca channels of vertebrate cells (Leung and Byerly, 1991), based on

their similarity to Ca channels in *Drosophila* neurons, which were shown to be insensitive to dihydropyridines (Byerly and Leung, 1988). In crayfish slow contracting skeletal muscle fibers, two Ca channels have been described with conductances of 14 and 38 pS (Bishop et al., 1991). Gating properties and voltage dependence of these channels have not been determined, but both are activated by depolarization. The mean open times of these Ca channels with about 40 ms for the 14 pS and 10 ms (judging from the published records) for the 38 pS channel, are, however, much longer than of the Ca channel reported here for fast contracting fibers. A Ca channel isolated from T-tubular membrane of crayfish skeletal muscle (of unknown type) and incorporated into lipid bilayers (Hurnák et al., 1990) has the DHP sensitivity of our Ca channel and a similar conductance, 16 pS, compared to 20 pS in our study. But again, the available data on the T-tubular channel is insufficient to allow a more detailed comparison, and different types of fibers may have different sets of Ca channels.

Comparison to Macroscopic Ca Currents

In the absence of Bay K8644, the macroscopic Ca current (Fig. 1, *D* and *E*) and quasimacroscopic Ba current (Fig. 2 *C*) is of the fast activating, fast deactivating type, as originally described for the L-type macroscopic Ca currents in a pituitary cell line (Matteson and Armstrong, 1986). In the single-channel records, fast deactivation shows in the absence of tail currents, i.e., channel openings after repolarization. The observation that there is no decline in single-channel activity either during voltage steps (Figs. 2 *B* and 9 *A*) or steady depolarization (Figs. 2 *A*, 7 *A*, and 10 *A*) nor any inactivation of the quasimacroscopic currents (Fig. 2 *C*) indicates that the sarcolemmal DHP-sensitive Ca channel in *Idotea* muscle does not inactivate voltage dependently. Based on voltage-clamp studies of Ca current inactivation in crayfish muscle, Ca channels in arthropod skeletal muscle were initially thought to inactivate voltage dependently, analogous to the classical Hodgkin-Huxley Na current (Hencek and Zachar, 1977). Later studies concluded that inactivation was either primarily Ca^{2+}-dependent (in insect muscle: Ashcroft and Stanfield, 1982; Salkoff and Wyman, 1983) or found a combined calcium-induced and voltage-dependent inactivation (in crab muscle: Mounier et al., 1988). Under physiological conditions, i.e. with Ca^{2+} instead of Ba^{2+} as charge carrier, our single channel data would only allow calcium-dependent inactivation for the macroscopic current through the sarcolemmal Ca channels. This view is supported by the large difference between the duration of Ca and Ba action potentials and the more rapid inactivation of the Ca over the Ba current (Fig. 1, *B–D*). Further investigation of the macroscopic Ca and Ba currents will have to show if the slow but clearly present inactivation of the macroscopic Ba current reflects a different population of Ca channels located in the T-system, or if other factors like ion depletion from the T-tubules (Almers et al., 1981; Ashcroft and Stanfield, 1982) can account for the difference between inactivation of the macroscopic and single-channel currents.

Dihydropyridine Sensitivity

The ability of the dihydropyridine (±) Bay K8644 to increase the frequency of long openings, a characteristic feature unique to L-type Ca channels, is the main argument for classification of the crustacean muscle Ca channel as L-type. Compared to mammalian cardiac muscle or nerve L-type channels, the sensitivity is quite low: at least 10 μM Bay K8644 was needed for a significant effect. However, a similarly high concentration of Bay K8644 (5 μM) seems to be required for the "slow" L-type Ca channel of vertebrate skeletal muscle, that was only recently characterized in its native membrane (Dirksen and Beam, 1995).

The sensitivity of mammalian L-type channels to the agonist S (−)-Bay K8644 is much higher than to the antagonist R (+)-Bay K8644, both of which constitute the racemic compound (±) Bay K8644 which is usually used. We also used the racemic compound and do not know the crustacean Ca channel's sensitivity ratio for agonist/antagonist. Sensitivity to the pure agonist could be higher.

Since we were unable to record from Ca channels in outside-out patches, we could not readily test the effects of DHP antagonists and peptide blockers on the sarcolemmal Ca channels. The current- and voltage-clamp experiments (Fig. 1), however, show that the macroscopic current is sensitive to DHP agonists and antagonists. The view that at least part of the Ca current in arthropod muscle is indeed through L-type Ca channels is also supported by a recent investigation on macroscopic currents in *Drosophila* larval muscle. Here, two types of current, resembling those through mammalian T- and L-type channels, have been resolved and pharmacologically analyzed (Gielow et al., 1995).

Voltage Sensitivity and Ion Selectivity

The average voltage sensitivity of the crustacean Ca channel of 8.2 mV depolarization required for an e-fold change in open probability is similar to the values reported, for example, for single L-type Ca channels in chick dorsal root ganglion neurons (5.5 mV) (Fox et al., 1987), whole-cell L-type currents in atrial myocytes (9.7 mV) (Bechem and Hoffmann, 1993), and DHP-sensitive skeletal muscle Ca channels in bilayers (6.9 mV) (Ma et al., 1991) or in the intact muscle (5.3 mV) (Dirksen and Beam, 1995). With L-type Ca channels of

smooth muscle from cerebral arteries, the crustacean Ca channel not only shares the voltage-sensitivity but also the range of half-maximal activation as well as single channel conductance (5–7 mV for e-fold change in P_o; $V_{0.5}$ = +13.5 mV and γ = 19.4 pS in 90 mM barium; Worley et al., 1991; Quayle et al., 1993).

Under our experimental conditions we did not see the shift in the activation curve (Fig. 8) to more negative potentials in the presence of Bay K8644 reported previously for macroscopic L-type Ca currents (Bechem and Hoffmann, 1993; Sanguinetti et al., 1986) or single-channel currents (Quayle et al., 1993). Since we recorded channel activity in cell-attached patches with unknown resting potential (see RESULTS), we would expect any such shift in the activation curve to be lost due to differences in the resting potentials of muscle fibers.

Ca Channel Gating Modes

During long-term recordings (Fig. 11) of the Ca channels, spontaneous shifts occurred between periods with openings and periods with no openings. Similarly, patches that initially did not seem to contain any channels often showed channel activity only after several minutes of recording. This switching between periods when the channel can be opened by depolarization and periods during which depolarization fails to elicit channel openings resembles the gating modes 1 and 0 described for L-type Ca channels of vertebrate ventricular cells (Hess et al., 1984). Similarly, the long openings, particularly evident in the presence of Bay K8644, might correspond — at least qualitatively — to mode 2 openings of Hess et al. (1984).

Physiological Consequences

What is the physiological function of the described sarcolemmal Ca channel? Since Ca^{2+} influx through the surface membrane (i.e., sarcolemma and transverse tubules) alone is probably unable to initiate contractions in crustacean muscle fibers (Mounier and Goblet, 1987), the sarcolemmal Ca channels cannot be directly responsible for muscle contraction. Furthermore, they are unlikely to even contribute directly to the CICR necessary for contraction since, in a large diameter muscle fiber like that of the crustacean, the sarcolemmal membrane is too far away from the sarcoplasmatic reticulum to allow for activation by Ca^{2+} diffusion. It seems instead that the sarcolemmal Ca channels are mainly for the electrogenic response which, in *Idotea* muscle fibers, can be either graded or regenerative in the form of action potentials (Erxleben et al., 1995). It seems likely, however, that the same L-type channel found in the sarcolemma by the single-channel recordings also exists in the T-tubules, since a large fraction of the macroscopic current is blocked by nifedipine (Fig. 1 *E*) and the activation and deactivation kinetics of quasimacroscopic single-channel and macroscopic currents are comparable (Figs. 1 and 2).

As discussed above, the data on the crustacean Ca channel presented here argue for it being L-type. One of the hallmarks of vertebrate L-type Ca channels is their susceptibility to modulation. Especially modulation that is mediated by phosphorylation through a cAMP/protein kinase A pathway is well established for vertebrate cardiac L-type channels (see, e.g., Hofmann et al., 1994; Campbell and Strauss, 1995) and neuronal L-type channels (see, e.g., Armstrong et al., 1991). The suggested identity of the crustacean Ca channel with L-type channels also makes it a likely target for modulation. Modulation leading to an increase in Ca current has in fact been observed in lobster skeletal muscle with octopamine and serotonin (Kravitz et al., 1980), and on the single-channel level, two calcium-permeable channels in flexor muscle fibers of the crayfish were shown to be up-regulated by proctolin (Bishop et al., 1991).

In conclusion, we have shown a voltage-dependent, dihydropyridine-sensitive L-type Ca channel in the sarcolemmal membrane of a crustacean muscle. Thus it appears that both vertebrate cardiac muscle and crustacean skeletal muscle may not only have a common mechanism of excitation-contraction coupling (a calcium-induced Ca^{2+} release) but also share the Ca channel type through which Ca influx occurs.

We thank Dr. David L. Armstrong for critically reading an early version of the manuscript and Mary A. Cahill for editorial assistance.

This work was supported by the Deutsche Forschungsgemeinschaft, SFB 156.

Original version received 23 July 1996 and accepted version received 29 November 1996.

REFERENCES

Almers, W., R. Fink, and P.T. Palade. 1981. Calcium depletion in muscle tubules: the decline of calcium current under maintained depolarization. *J. Physiol. (Lond.).* 312:177–207.

Araque, A., and W. Buño. 1995. Fast, persistent, Ca^{2+}-dependent K^+ current controls graded electrical activity in crayfish muscle. *Pflüg. Arch. Eur. J. Physiol.* 430:541–551.

Armstrong, D.L., M.F. Rossier, A.D. Shcherbatko, and R.E. White. 1991. Enzymatic gating of voltage-activated calcium channels.

Ann. NY Acad. Sci. 635:26–34.

Ashcroft, F.M., and P.R. Stanfield. 1982. Calcium inactivation in skeletal muscle fibers of the stick insect, *Carausius morosus*. *J. Physiol. (Lond.).* 330:349–372.

Bean, B.P. 1992. Whole-cell recording of calcium channel currents. *In* Methods in Enzymology. B. Rudy and L.E. Iverson, editors. Academic Press, Inc., San Diego, CA. 181–193.

Bechem, M., S. Hebisch, and M. Schramm. 1988. Ca^{2+} agonists: new, sensitive probes for Ca^{2+} channels. *Trends Pharmacol. Sci.* 9: 257–261.

Bechem, M., and H. Hoffmann. 1993. The molecular mode of action of the Ca agonist (-) BAY K 8644 on the cardiac Ca channel. *Pflüg. Arch. Eur. J. Physiol.* 424:343–353.

Bishop, C.A., M.E. Krouse, and J.J. Wine. 1991. Peptide cotransmitter potentiates calcium channel activity in crayfish skeletal muscle. *J. Neurosci.* 11:269–276.

Byerly, L., and H.-T. Leung. 1988. Ionic currents of *Drosophila* neurones in embryonic cultures. *J. Neurosci.* 8:4379–4393.

Campbell, D.L., and H.C. Strauss. 1995. Regulation of calcium channels in the heart. *Adv. Second Messenger Phosphoprotein Res.* 30: 25–88.

Colquhoun, D., and F.J. Sigworth. 1983. Fitting and statistical analysis of single-channel records. *In* Single-channel Recording. B. Sakmann and E. Neher, editors. Plenum Press, New York. 191–263.

Deitmer, J.W., and W. Rathmayer. 1976. Calcium action potentials in larval muscle fibres of the moth *Ephestia kühniella* Z. (Lepidoptera). *J. Comp. Physiol.* 112:123–132.

Dirksen, R.T., and K.G. Beam. 1995. Single calcium channel behavior in native skeletal muscle. *J. Gen. Physiol.* 105:227–247.

Erxleben, C.F.J., A. deSantis, and W. Rathmayer. 1995. Effects of proctolin on contractions, membrane resistance, and non-voltage-dependent sarcolemmal ion channels in crustacean muscle fibers. *J. Neurosci.* 15:4356–4369.

Fabiato, A. 1985. Time and calcium dependence of activation and inactivation of Ca-induced release of Ca from the SR of a skinned canine cardiac Purkinje cell. *J. Gen. Physiol.* 85:247–289.

Fatt, P., and B.L. Ginsborg. 1958. The ionic requirements for the production of action potentials in crustacean muscle fibres. *J. Physiol. (Lond.).* 142:516–543.

Fatt, P., and B. Katz. 1953. The electrical properties of crustacean muscle fibers. *J. Physiol. (Lond.).* 120:171–204.

Fox, A.P., M.C. Nowycky, and R.W. Tsien. 1987. Single-channel recordings of three types of calcium channels in chick sensory neurones. *J. Physiol. (Lond.).* 394:173–200.

Gainer, H. 1968. The role of calcium in excitation-contraction coupling of lobster muscle. *J. Gen. Physiol.* 52:88–110.

Gielow, M.L., G.-G. Gu, and S. Singh. 1995. Resolution and pharmacological analysis of the voltage-dependent calcium channels of *Drosophila* larval muscles. *J. Neurosci.* 15:6085–6093.

Gilly, W.F., and T. Scheuer. 1984. Contractile activation in scorpion striated muscle fibers. Dependence on voltage and external calcium. *J. Gen. Physiol.* 84:321–345.

Goblet, C., and Y. Mounier. 1986. Calcium-induced Ca release mechanism from the SR in skinned crab muscle fibres. *Cell Calcium.* 7:61–72.

Györke, S., and P. Palade. 1992. Calcium-induced calcium release in crayfish skeletal muscle. *J. Physiol. (Lond.).* 457:195–210.

Hagiwara, S., and K.-I. Naka. 1964. The initiation of spike potential in barnacle muscle fibers under low intracellular Ca^{++}. *J. Gen. Physiol.* 48:141–162.

Hagiwara, S., K. Takahashi, and D. Junge. 1968. Excitation-contraction coupling in a barnacle muscle fibre as examined with voltage clamp techniques. *J. Gen. Physiol.* 51:157–175.

Hencek, M., and J. Zachar. 1977. Calcium currents and conductances in the muscle membrane of the crayfish. *J. Physiol. (Lond.).* 268:51–71.

Hess, P., J.B. Lansman, and R.W. Tsien. 1984. Different modes of Ca channel gating behaviour favored by dihydropyridine Ca agonists and antagonists. *Nature (Lond.).* 311:538–544.

Hidalgo, J., M. Luxoro, and E. Rojas. 1979. On the role of extracellular calcium in triggering contraction in muscle fibres from barnacle under membrane potential control. *J. Physiol. (Lond.).* 288: 313–330.

Hodgkin, A.L. 1951. The ionic basis of electrical activity in nerve and muscle. *Biol. Rev. Camb. Philos. Soc.* 26:339–409.

Hofmann, F., M. Biel, and V. Flockerzi. 1994. Molecular basis for Ca^{2+} channel diversity. *Annu. Rev. Neurosci.* 17:399–418.

Hurnák, O., P. Proks, O. Krizanová, and J. Zachar. 1990. DHP-sensitive Ca^{2+} channels from crayfish skeletal muscle T-tubules incorporated into planar lipid bilayers. *Gen. Physiol. Biophys.* 9:643–646.

Kunze, D.L., and A.K. Ritchie. 1990. Multiple conductance levels of the dihydropyridine-sensitive calcium channel in GH_3 cells. *J. Membr. Biol.* 118:171–178.

Kravitz, E.A., S. Glusman, R.M. Harris-Warrick, M.S. Livingstone, T. Schwarz, and M.F. Goy. 1980. Amines and a peptide as neurohormones in lobsters: actions on neuromuscular preparations and preliminary behavioural studies. *J. Exp. Biol.* 89:159–175.

Lacerda, A.E., and A.M. Brown. 1989. Nonmodal gating of cardiac calcium channels as revealed by dihydropyridines. *J. Gen. Physiol.* 93:1243–1273.

Lea, T.J., and C.C. Ashley. 1989. Ca-induced Ca release from the sarcoplasmic reticulum of isolated myofibrillar bundles of barnacle muscle fibres. *Pflüg. Arch. Eur. J. Physiol.* 413:401–406.

Leung, H.-T., and L. Byerly. 1991. Characterization of single calcium channels in *Drosophila* embryonic nerve and muscle cells. *J. Neurosci.* 11:3047–3059.

Ma, J., C. Mundiña-Weilenmann, M.M. Hosey, and E. Ríos. 1991. Dihydropyridine-sensitive skeletal muscle Ca channels in polarized planar bilayers. 1. Kinetics and voltage dependence of gating. *Biophys. J.* 60:890–901.

Matteson, D.R., and C.M. Armstrong. 1986. Properties of two types of calcium channels in clonal pituitary cells. *J. Gen. Physiol.* 87:161–182.

Mounier, Y., and C. Goblet. 1987. The role of different calcium sources in the excitation-contraction coupling in crab muscle fibres. *Can. J. Physiol. Pharmacol.* 65:667–671.

Mounier, Y., V. Stal, and C. Goblet. 1988. Calcium-induced and voltage-dependent inactivation of calcium channels in crab muscle fibres. *Gen. Physiol. Biophys.* 7:113–134.

Quayle, J.M., J.G. McCarron, J.R. Asbury, and M.T. Nelson. 1993. Single calcium channels in resistance-sized cerebral arteries from rats. *Am. J. Physiol.* 264:H470–H478.

Salkoff, L.B., and R.J. Wyman. 1983. Ion currents in *Drosophila* flight muscles. *J. Physiol. (Lond.).* 337:687–709.

Sanguinetti, M.C., D.S. Krafte, and R.S. Kass. 1986. Voltage-dependent modulation of Ca channel current in heart cells by Bay K8644. *J. Gen. Physiol.* 88:369–392.

Washio, H. 1972. The ionic requirements for the initiation of action potentials in insect muscle fibers. *J. Gen. Physiol.* 59:121–134.

Worley, J.F., J.M. Quayle, N.B. Standen, and M.T. Nelson. 1991. Regulation of single calcium channels in cerebral arteries by voltage, serotonin, and dihydropyridines. *Am. J. Physiol.* 261:H1951–H1960.

Zacharová, D., and J. Zachar. 1967. The effect of external calcium ions on the excitation-contraction coupling in single muscle fibres of the crayfish. *Physiol. Bohemoslov.* 16:191–207.